SciMedCentral

JSM Clinical Case Reports

Case Report

Biological Properties of a Benzotiazole-Based Mononuclear Platinum(II) Complex as a Potential Anticancer Agent

Zhanfen Chen*, Yixuan Wu, Qiang Zhang and Yumin Zhang

Flexible Display Mater & Tech, Co-Innovation Center of Hubei,Key Laboratory of Optoelectronic Chemical Materials and Devices of Ministry of Education,School of Chemistry and Environmental Engineering,Jianghan University, People's Republic of China

***Corresponding author**

Zhanfen Chen, Flexible Display Mater. & Tech, Co-Innovation Center of Hubei,Key Laboratory of Optoelectronic Chemical Materials and Devices of Ministry of Education,School of Chemistry and Environmental Engineering, Jianghan University,Wuhan 430056, People's Republic of China, Email: chenzf1979@163.com

Submitted: 05 April, 2020

Accepted: 30 April, 2020

Published: 11 May, 2020

ISSN: 2373-9819

OPEN ACCESS

Abstract

A novel mononuclear platinum(II) complex, [PtLCl]Cl (1, where L N-(4-(benzo[d]thiazol-2-yl)phenyl)-2-(bis(pyridine-2-ylmethyl)-amino)acetamide), was synthesized by covalently tethering a benzothiazole derivative 2-(4-aminophenyl)benzothiazole to the 2,2'-dipicolylamine (DPA) chelating PtII center by an amidic bond. The complex showed a cytotoxicity comparable to that of cisplatin against MCF-7 cell lines, and more potent activities against HeLa and A-549 cell lines. Investigations of the reaction of 1 with 5'-GMP display that 1 could coordinate with N7-GMP to form the Pt-GMP adduct. Thus 1 has potential to form Pt-DNA adducts in vivo. Similarly, the glutathione (GSH) ligand could also coordinate to the Pt(II) center to form a monodentatePt-GS complex. The competition experiments of 1 with 5'-GMP and GSH showed that the coordination binding of 1 with GSH did not prevent the formation of a certain amount of the Pt-GMP adduct in the reaction process. DNA binding experiments displayed that 1 could bind to DNA through multiple binding modes involving non-covalent interaction and monofunctionalplatination of the platinum(II) moiety, and induce a visible conformational change of DNA. The evaluation of the protein binding ability showed that complex 1 could bind to human serum albumin (HSA) with a moderate binding affinity, quench the intrinsic fluorescence of HSA, and destroy the tertiary structure of HSA.

INTRODUCTION

Platinum-based anticancer drugs are the predecessor of inorganic chemotherapeutic drugs for the treatment of various malignant cancer types. However, the severe side effects and inevitable drug resistance have limited their clinical application [1,2]. In our endeavor to explore new possible anticancer drug candidates, we recently show that the introduction of planar aromatic ligands or biologically active carrier group to the Pt coordination moiety is an effective strategy, which is in favor of increasing DNA binding ability and enhancing the cytotoxicity [3,4]. This class of platinum(II) compounds, unlike cisplatin, do not induce cross-links but target DNA through multiple binding modes involving non-covalent interaction and the monofunctional platination of nucleobase nitrogen [3-5]. Because of the synergic action, they often produced more detrimental effect to a cell's replisome and transcription than cisplatin and demonstrated excellent cytotoxicity against some solid tumor cells. So they have the great pharmacological potential as new therapeutic agents.

Benzothiazole and its derivatives are the important heterocyclic compounds, which play a significant role in medicinal chemistry and have diverse biological effects, such as antimicrobial, anticancer, anticonvulsant, antiviral, anti-inflammatory, anthelmintic, antibacterial, antioxidant, and antidiabetic activity [6-8]. They have been extensively used in the clinic in preventing and treating various types of diseases with low toxicity, high bioavailability, and good biocompatibility and curative effects. Based on the unique properties, medicinal chemists or biochemists have drawn their attention to introducing the benzothiazolepharmacophore moiety into anticancer drug design to clinically realize the conception of combined anticancer therapies or multi-acting drugs. For example, a fluorescent rhenium complex conjugated to 2-(3-aminophenyl)benzothiazoles has been introduced as a promising radiopharmaceutical candidate for breast cancer [9,10]. A gadolinium complex based on the conjugate of 1,4,7,10-tetraazacyclododecane-1,4,7-trisacetic acid and benzothiazole aniline was reported be a single molecule theranostic agent [11]. A series of triazole and isoxazole tagged benzothiazole derivatives induced an increase in expression of key apoptotic genes that are involved in the intrinsic pathway of apoptosis such as caspase-9, caspase-3, BAX and cytochrome-c and displayed very significant cytotoxic activity against human cancer cell lines [12]. However, the report of tethering benzothiazole or its derivatives to platinum chelating fragments to develop platinum-based anticancer drugs with potent cytotoxicity or multimodal therapeutic functionality is very limited. As a continuation to our efforts for identifying new

potent and multimodal anticancer agents, a novel mononuclear platinum(II) complex (1) was constructed by covalently tethering a planar benzothiazole derivative 2-(4-aminophenyl)benzothiazole to the 2,2′-dipicolylamine (DPA) chelating PtII center by an amidic bond, its structure depicted in Scheme 1, and was investigated the anticancer potential.

It is well-known that the cytotoxicity of platinum-based antitumor drugs stems from their binding to DNA and formation of covalent cross-links [13]. This means that DNA is the primary target for platinum-based anticancer agents. Hence, the interaction investigation of active platinum complexes with DNA, its model compound guanosine-5′-monophosphate (5′-GMP), and its interferent substance glutathione (GSH) is a fundamental issue in the development of platinum-based anticancer drugs, which provide some valuable information on the replication, transcription, and mutation of genes and the related variations of species in character, origin of some disease and mechanism of exerting pharmacological activity [14]. Additionally, protein is also considered to be one of the targets in the action of anticancer agents, which is believed to contribute to drug unwanted side-effects, drug resistance, and even possibly drug delivery and storage [15]. Therefore, in the paper, we investigated the cytotoxicity, DNA binding ability, reactivity with 5′-GMP and GSH, and human serum albumin (HSA) interaction of complex 1 (Scheme 1).

EXPERIMENTAL SECTION

Materials and methods

N-(4-(benzo[d]thiazol-2-yl)phenyl)-2-chloroacetamide and 2,2′-dipicolylamine (DPA) were synthesized following the published procedures [3,16]. K2PtCl4 was obtained from Shandong BoyuanParmaceutical Co. Ltd. cis-Pt(DMSO)$_2$Cl$_2$ was synthesized from K2PtCl4 as previous reported [17]. Calf thymus DNA (CT-DNA), tris(hydromethyl)aminomethane (Tris), ethidium bromide (EB), 5′-GMP sodium salt, glutathione (GSH), and human serum albumin (HSA, agarose gel electrophoresis, lyophilized powder, product number 1653, 96-99%) were purchased from Sigma and used without further purification. All the other chemicals and reagents were of analytical grade and used as received without further purification. Water used in the study was doubly distilled deionized.

IR spectra (as KBr pellets) were recorded in the range of 500-4000 cm^{-1} with a Nicolet 5700 FT-IR spectrometer. Elementary analyses were carried out on a Perkin-Elmer 2400 analytical instrument. Electrospray mass spectra were obtained on an LCQ electrospray mass spectrometer (ESI-MS, Finnigan). The isotopic distribution patterns for the complexes were simulated using the ISOPRO 3.0 program [18]. 1H NMR experiments were performed on a Bruker Advance 300 NMR spectrometer at 298 K using standard pulse sequences. UV-vis absorption spectra were measured on a Hitachi U-3010 UV-vis spectrophotometer using matched quartz cuvettes (1.0 cm). Fluorescence determination was carried out on a Hitachi F-4500 spectrofluorophotometer. The circular dichroism (CD) spectra were acquired on a Jasco J-810 spectropolarimeter (Japan Spectroscopic, Japan).

Synthesis of N-(4-(benzo[d]thiazol-2-yl)phenyl)-2-(bis(pyridine-2-ylmethyl)-amino)acetamide (L)

The ligand N-(4-(benzo[d]thiazol-2-yl)phenyl)-2-(bis(pyridine-2-ylmethyl)-amino)acetamide (L) was synthesized using a published method with some modifications [3]. N-(4-(Benzo[d]thiazol-2-yl) phenyl)-2-chloroacetamide (3.02 g, 10 mmol), K_2CO_3 (1.38 g, 10 mmol), DPA (1.99 g, 10 mmol), and KI (0.2 g, 1.2 mmol) were mixed in 80 mL of acetonitrile. The mixture was stirred and refluxed for 24 h, and filtered. The filtrate was concentrated under reduced pressure and purified with silica gel chromatography (dichloromethane/ethyl acetate, v/v, 1:5) to obtain a white power product. Yield: 40%. Elemental anal.found (calc.) for $C_{27}H_{23}N_5SO$ (%): C 69.54 (69.68); H 4.89 (4.95); N 15.13 (15.05). ESI-MS (*m/z*, methanol): 466.27 [M + H]$^+$; 931.40 [2M + H]$^+$; 953.13 [2M + Na]$^+$. 1H NMR (300 MHz, $CDCl_3$, δ, ppm): 8.64 (2H, d, J = 4.3 Hz), 8.08 (2H, m, J = 14.8 Hz), 7.96 (2H, d, J = 8.4 Hz), 7.87 (2H, t, J = 8.6 Hz), 7.65 (2H, t, J= 7.9 Hz), 7.48-7.36 (2H, m, J = 9.8 Hz), 7.27 (2H, t, J= 7.7 Hz), 7.18 (2H, t, J= 7.6 Hz), 3.95 (4H, s), 3.51 (2H, s). FT-IR (KBr pallet, v/cm^{-1}): 3447 (vs), 1661 (s), 1588 (m), 1540 (m), 1512 (m), 1433 (m), 832 (m), 751 (m).

Synthesis of [PtLCl]Cl (1)

The complex was prepared by the following procedures. The ligand L (0.18 g, 0.4 mmol) was dissolved in methanol, whose pH value was adjusted to 7-8 with 1 M NaOH. The solution was added to a methanol solution of cis-Pt(DMSO)2Cl$_2$ (0.17 g, 0.4 mmol). The mixture solution was refluxed and stirred for 24 h and concentrated under reduced pressure. The residue was filtrated, washed with acetone and diethyl ether, and dried in vacuo to give light yellow powder product. Elemental anal.found (calc.) for PtC27H23N5SOCl2 (%): C, 44.46 (44.32); H, 3.25 (3.15); N, 9.62 (9.58). ESI-MS (*m/z*, methanol): 696.47 [M -Cl]$^+$; 1390.20 [2M - 2Cl -H]$^+$. FT-IR (KBr pallet, v/cm^{-1}): 3412 (*vs*), 3035 (m), 2359 (m), 1603 (vs), 1535 (m), 1478 (s), 1441 (m), 1311 (m), 768 (s).

Cytotoxicity

The cytotoxicity of [PtLCl]Cl (1), L, and cisplatin was screened against the human cervical cancer cell line HeLa, the human non-small-cell lung cancer cell line A-549, and the human breast cancer cell line MCF-7 by the MTT assay. Briefly, tumor cells were inoculated in 96-well plates and incubated in medium overnight. A stock solution of cisplatin was prepared in PBS and complex 1 and L were dissolved in DMSO, respectively. The stock solutions were diluted in medium to make the concentration of DMSO lower than 0.5% and then added to per well. The cells were incubated for 48 h, and aliquot MTT solution (20 μL, 5 mg mL^{-1} in PBS) was added to each well. After incubation for 4 h, the supernatant was removed and DMSO (200 μL) was added to solubilize the MTT formazan. The amount of MTT formazan was determined using a Tecan Sunrise ELISA Reader at 570 nm after the plates were shaking for 30 min. The optical density (OD) was used to calculate the percentage of cell viability relative to the untreated control values, that is, (ODcontrol-ODtest)/(ODcontrol-ODblank) × 100%. The background readings of MTT incubated in a cell-free medium were subtracted from each value before calculation. The half-maximal inhibitory concentration (IC_{50}) of the compounds was obtained from the fitted inhibition curves at 48 h. The mean IC_{50} was calculated using the data from three replicates.

Reactivity with 5′-GMP and GSH

The reactivity of complex 1 with 5′-GMP and GSH was investigated using electrospray mass spectrometry (ESI-MS). The

samples were prepared by reacting complex 1 with an equivalent of 5-GMP or GSH or their mixture in methanol/water (v/v, 1:1) at 37 °C for 24 h before electrospraying in the positive ion mode.

DNA binding ability

CT-DNA stock solution was prepared with Tris-HCl buffer solution (5 mMTris, 50 mMNaCl, pH 7.4), which was stored at 4 °C overnight and used within one week. The concentration of CT-DNA was determined by measuring the UV absorption at 260 nm, taking 6600 M^{-1} cm^{-1}as the molar absorption coefficient (ε_{260}) [19]. The stock solution of complex 1 was prepared with 10% DMSO and 90% buffer (5 mMTris, 50 mMNaCl, pH 7.4). The concentration of the complex was eventually reduced to 40 μM while adding the calculated amounts of DNA (20 μM, r = [CT-DNA]/[complex] = 0.5), and the final volume of the solution were fixed to 3 mL. The UV-vis absorption spectra of the mixture solution were recorded after 1 min, 3 h, 6 h, 9 h, 12 h, respectively. It has been verified that a low DMSO percentage added to the DNA solution would not interfere with the nucleic acid [20].

The fluorescence spectra of complex 1 (λ_{ex}= 360 nm, λ_{em}= 380-520 nm) in the absence and presence of CT-DNA (r= [DNA]/[1] = 0.1, 0.2, 0.3, 0.4, 0.5, 0.6, 0.7, 0.8, 0.9) were recorded at room temperature after 24 h of incubation. The influence of 1 on the EB-DNA complex ([DNA] = [EB] = 1.136 × 10^{-5} M) was measured by recording the variation of fluorescence emission spectra (λ_{ex}= 526 nm, λ_{em}= 540-750 nm).

CD spectra of CT-DNA in the absence and presence of complex 1 were recorded in the range of 220-320 nm using a scan speed of 10 nm min^{-1} at room temperature and the buffer background was subtracted.

Interaction studies with protein

HSA stock solution was prepared by dissolving solid HSA in Tris-HCl buffer (0.05 M Tris-HCl/0.1 M NaCl, pH 7.40), which is stored at 0-4' and used within a week. The stock solution of 1 was prepared with 10% DMSO and 90% buffer (0.05 M Tris-HCl/0.1 M NaCl, pH 7.40). Fluorescence measurements were carried out maintaining a fixed HSA concentration (0.4 μM) in a quartz cell while varying the concentration of complex 1 (1.5-120 μM). An excitation wavelength of 280 nm was selected and the emission wavelength was recorded from 280-500 nm after the mixtures equilibrating for 24 h at the appropriate temperature (291, 299, 309 K). Both excitation and emission band widths were set on 2.5 nm. The data obtained were analyzed using the Stern-Volmer and modified double logarithm regression equations. For synchronous fluorescence measurements, the excitation range was 250-310 nm, and the scanning interval between excitation and emission wavelengths (Δλ) was set on 15 or 60 nm.

The absorption spectra of HSA (1.0 μM) were recorded in the absence and presence of increasing amounts of complex 1 (0.5-5.0 μM) at 37 in pH 7.40 after 24 h of incubation time. In order to eliminate the absorption of complex 1 itself, an equal amount of 1 was subsequently used as reference. The CD spectra of HSA in the presence of 1 were recorded over the range of 200-260 nm, taking the average of three scans as the final data for each spectrum.

RESULTS AND DISCUSSION

Synthesis of L and [PtLCl]Cl (1)

The novel ligand L was obtained using a similar literature method [3], and fully characterized by ESI mass spectrometry, NMR spectroscopy, elementary analyses, and IR spectra (Figures S1, S2 in the ESI). The platinum(II) complex [PtLCl]Cl (1) was synthesized by reacting L and cis-$Pt(DMSO)_2Cl_2$ in methanol. The formation of the mononuclear platinum(II) complex was confirmed by ESI-MS. The ESI-MS spectrum of complex 1 in methanol solution gave two signals at m/z 696.47 and 1390.20 (Figure S3), which could be assigned to $[PtLCl]^+$ ($PtC_{27}H_{23}N_5SOCl$) and $[2(PtLCl) - H]^+$ ($Pt_2C_{54}H_{45}N_{10}S_2O_2Cl_2$), respectively. The isotopic distribution pattern of the peaks matched perfectly with the simulated one. The signal of $[PtLCl]^+$ still existed after about 4 days, indicating that complex 1 is stable in methanol solution.

Cytotoxicity

Cytotoxicity of [PtLCl]Cl (1) and L was tested against HeLa, A-549, and MCF-7 cell lines. Cisplatin was used as a positive reference. The IC_{50} values are presented in Table 1. As shown in Table 1, complex 1 exhibits a cytotoxicity comparable to that of cisplatin against MCF-7 cell line, and more potent activities against HeLa and A-549 cell lines. However, the ligand L shows moderate cytotoxic activity towards the three tested cell lines, which indicates that an evident increase in the cytotoxicity of 1 compared to its ligand L should result from the coordination of Pt(II).

Reaction of complex 1 with 5'-GMP and GSH(Figure 1)

Guanine-N7 is the preferred binding site in DNA for platinum-based anticancer drugs [21]; therefore, the reactivity of complex 1 with a model compound 5'-GMP at a 1:1 molar ratio was monitored by ESI-MS spectroscopy. Complex 1 and 5'-GMP were incubated in methanol/water (v/v, 1:1) at 37 for 24 h, and then the mixture was subjected to ESI-MS determination. As shown in Fig. 1, the ESI-MS spectrum gave two peaks at m/z 696.27 and 1022.40, respectively. The peak at m/z 696.27 was assigned to unreacted [PtLCl]+ ($C_{27}H_{23}N_5OSClPt$), and the peak at m/z1022.40 should be ascribed to the positively charged species $[PtL(GMP) - 2Na + H]^+$ ($C_{37}H_{36}N_{10}O_9SPPt$), which was formed by complex 1 and 5'-GMP after losing a chloride ion. The result indicates that complex 1 could (Figure 2)react readily with 5'-GMP to form 1:1 adduct and has the potential to form monofunctionalPt-DNA adducts in vivo.

Sulfur-containing molecules play significant roles in the anticancer mechanism of platinum drugs [22]. Glutathione (GSH) is one of the most abundant intracellular sulfur-containing molecules and its role in platinum anticancer chemotherapy appears to be dual, namely that it deactivates as well as activates the drugs [22,23]. Due to

Table 1: Cytotoxicity of [Pt**L**Cl]Cl (**1**) and L (48 h).

Tested compound	IC_{50}[a] (mM)		
	HeLa	A-549	MCF-7
Cisplatin	6.19 ± 0.2	9.10 ± 0.2	4.61 ± 1. 2
Complex **1**	4.23 ± 0.6	5.52 ± 0.7	15.45 ± 0. 2
L	69.59 ± 1.3	59.12 ± 1.2	55.21 ± 1.5

[a] Compound concentration required to inhibit cell proliferation by 50%.

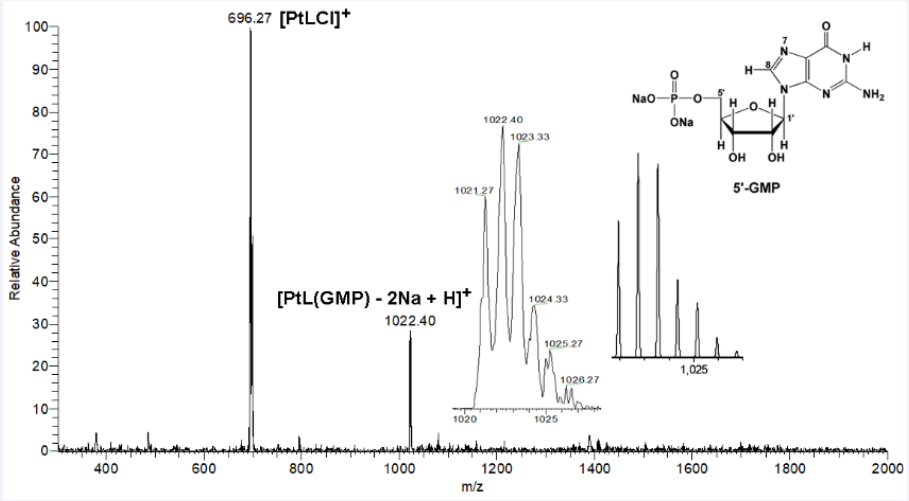

Figure 1 ESI-MS spectrum (positive mode) of the reaction between complex **1** and 5′-GMP (1:1) recorded in methanol/water (v/v, 1:1) at 37 °C for 24 h. Assignments: 1022.40, [Pt**L**(GMP) – 2Na + H]+ ($C_{37}H_{36}N_{10}O_9SPPt$, calcd 1022.87); 696.27, [Pt**L**Cl]+ ($C_{27}H_{23}N_5OSClPt$, calcd 696.12).

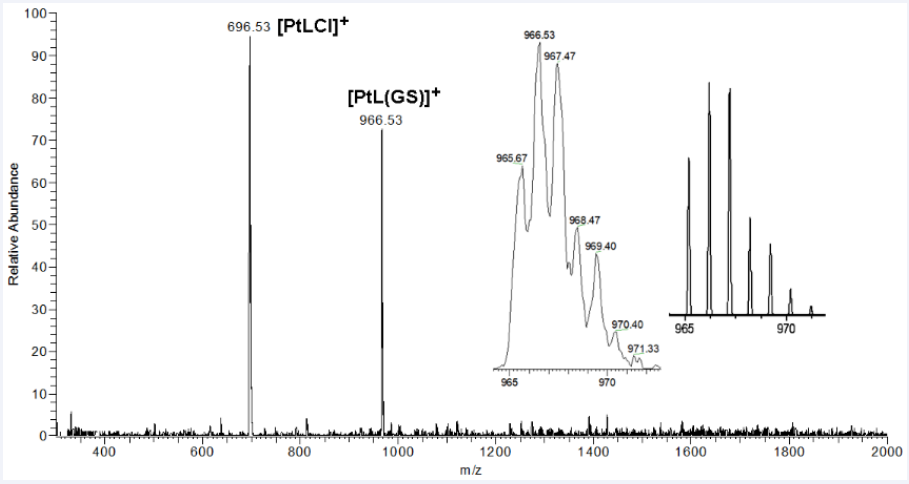

Figure 2 ESI-MS spectrum (positive mode) of the reaction between complex **1** and GSH (1:1) recorded in methanol/water (v/v, 1:1) at 37 °C for 24 h. Assignments: 966.53, [Pt**L**(GS)]+ ($C_{37}H_{39}N_8O_7S_2Pt$, calcd 966.97); 696.53, [Pt**L**Cl]+ ($C_{27}H_{23}N_5OSClPt$, calcd 696.11).

its significant biological role, the reactivity of complex 1 toward GSH was investigated by ESI-MS. After the incubation of complex 1 with an equivalent of GSH in methanol/water (v/v, 1:1) at 37 for 24 h, two peaks were observed in the ESI-MS spectrum (Figure 2). The peak at m/z 696.53 was assigned to unreacted [PtLCl]+ ($C_{27}H_{23}N_5OSClPt$) and the peak at *m/z* 966.53 should be ascribed to the positively charged species [PtL(GS)]+ ($C_{37}H_{39}N_8O_7S_2Pt$). The result suggests that one GSH ligand could be coordinated to the Pt(II) center to form a monodentatePt-GSH complex.

Furthermore, we studied the competitive reaction of complex 1 with GSH and 5'-GMP by ESI-MS spectroscopy. Electrospraying a mixture of the three compounds at a relative proportion of Pt(II)/GSH/5'-GMP of 1:1:1 in the positive ion mode after 24 h incubated time, generated the mass spectrum shown in Fig. S4. The peaks of the monodentatePt-GS adduct [PtL(GS)]+ (*m/z*, 966.67) and the Pt-GMP adduct [PtL(GMP)-2Na + H]+ (m/z, 1022.67) were observed in the spectrum with 100% intensity (in % relative to the highest peak) and 55% intensity, respectively. And the unreacted [PtLCl]+ peak was not observed in the spectrum. The result indicated that after 24 h, complex 1 had run out in the reaction medium to form the Pt-GS adduct and the Pt-GMP adduct and the coordination binding of complex 1 with GSH did not prevent the formation of a certain amount of the Pt-GMP adduct in the reaction process, which was in agreement with our previously published results [3].

DNA binding ability (Figure 3)

DNA binding ability of 1 was investigated using UV-vis absorption, fluorescence, and CD spectroscopy. The time-dependent UV absorption spectra of 1 (40 μM) in the absence and presence of CT-DNA (20 μM) are shown in Figure 3. It is found that the absorption bands at 310 nm of complex 1, which is attributed to the metal to ligand charge transfer (MLCT), displays a significant decrease in intensity as time grows. After 12 h, a 20% hypochromism is observed, which is much larger than that observed for most DNA intercalators, suggesting that 1 could strongly bind to DNA [24] (Figure 4(a), 4(b))

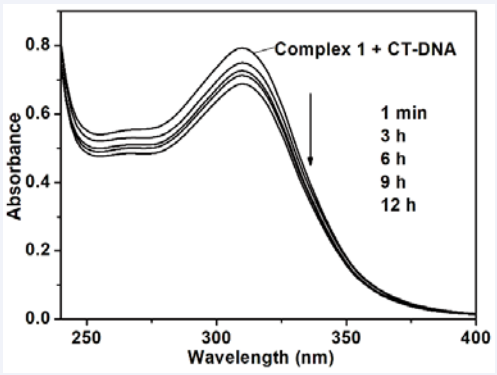

Figure 3 Time-dependent absorption spectra of **1** (40 μM) in the presence of a fixed amount of CT-DNA (*r* = [DNA]/[complex] = 0.5) at room temperature in pH 7.40.

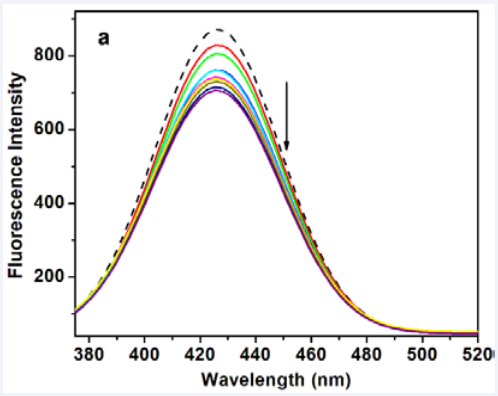

Figure 4a Fluorescence emission spectra of complex **1** (0.3 μM, λ_{ex} = 360 nm) in the absence (dashed line) and presence (solid lines) of CT-DNA (*r* = [DNA]/[**1**] = 0.1, 0.2, 0.3, 0.4, 0.5, 0.6, 0.7, 0.8, 0.9) at 37 °C after 24 h of incubation;

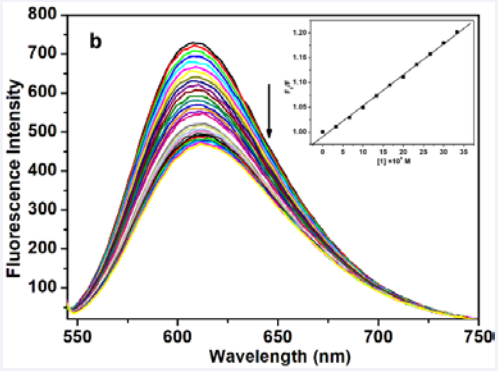

Figure 4b Fluorescence emission spectra (λex = 526 nm) of the CT-DNA-EB system ([DNA] = [EB] = 1.136 × 10−5 M) in the absence and presence of complex 1 (1.0 × 10−3 M, 10 μL per scan). Inset: the Stern-Volmer plot of the EB-DNA fluorescence titration for complex 1.

The fluorescence spectra of 1 in the absence and presence of CT-DNA are shown in Figure 4(a). The complex possesses intense fluorescence with emission and excitation maxima at 426 nm and 360 nm, respectively. Upon the incremental addition of DNA, the fluorescence emission intensity of 1 gradually decreases, implying that 1 can bind to DNA and quench the native fluorescence. To further clarify the interaction pattern of the complex with DNA, fluorometric competitive binding experiments were carried out using EB, a known DNA intercalator that causes a significant increase in the fluorescence intensity when bound to DNA and its displacement from the DNA-EB adduct leads to a dramatic decrease in the intensity [25]. The fluorescence emission spectra of the EB-DNA system in the absence and presence of 1 are shown in Figure 4(b). As shown in Figure 4(b), the fluorescence emission intensity at about 608 nm (λ_{ex}= 526 nm) decreases obviously with titration of the complex to the EB-DNA system and finally reaches saturation, indicating the partial removal of EB from DNA molecules due to the interaction of the complex with DNA. The inset of Figure 4(b) shows the plot of *F0/Fvs*. [complex], which exhibits good linear correlation with high R values (R = 0.9984, the correlation coefficient) within the quenching concentration range, and suggests that the fluorescence quenching curve of DNA-bound EB by 1 is in good agreement with linear Stern-Volmer equation. The quenching constant (Ksv) of 6.2 ×103 M^{-1} was obtained from the slope of the linear plot, indicating a strong binding affinity of 1 to CT-DNA [26]. Furthermore, from the plot of *F0/F vs*. [complex], the apparent DNA binding constant (Kapp) was calculated using the following equation [27]:

$$K_{EB}[EB]=K_{app}[complex] \quad (1)$$

where KEB is the DNA binding constant of EB (KEB = 1.0 ×107 M^{-1}), [EB] is the concentration of EB (1.136 × 10^{-5}M), and [complex] is the concentration of the complex at 50% reduction of the initial fluorescence emission intensity of EB [28]. The values of Kapp are 7.06 ×105 M^{-1}, which is less than the binding constant of the classical intercalators and metallointercalators (10^7 M^{-1}) and is in the range of 10^4-10^5 M^{-1}[29,30]. The results show that DNA binding of the complexes might be mainly by the groove binding mode. Since the planar 2-(4-aminophenyl)benzothiazole aromatic ring exists in the ligand system of 1, which maybe favor intercalation of the complex between base pairs of DNA, intercalation binding mode could not be ruled out in the interaction between the complex and DNA. Moreover, considering its high reactivity towards 5-GMP, a covalent binding to DNA is highly possible, which would greatly affect the conformation of DNA (Figure 5).

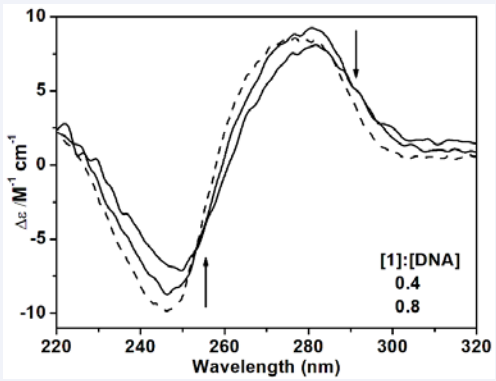

Figure 5 CD spectra of CT-DNA (0.1 mM, dashed line) under the influence of complex 1 at concentration ratios of complex to DNA of 0.4 and 0.8.

The conformational change of CT-DNA is measured using circular dichroism (CD) spectroscopy. Figure 5 displays the CD spectra of CT-DNA in the absence and presence of varying amounts of complex 1 ([1]/[DNA] = 0.4, 0.8). It is known that, the positive absorption band at about 275 nm and the negative one at about 245 nm in the CD spectrum of free CT-DNA (dashed lines) are due to the base stacking and the right-handed helicity of B-DNA, respectively [31]. The simple groove binding or electrostatic interaction between small molecules and DNA causes less or perturbation on the base stacking and helicity bands, whereas a classical intercalation can stabilize the helix conformation of B-DNA, and enhances the intensities of both the CD bands, as observed for the classical intercalator methylene blue [32]. When treated with 1, the positive bands decreased generally in ellipticity with obvious redshifts and the negative band ellipticity decreased obviously with a significant red shift. The result showed that the complex could bind to CT-DNA and the interaction could disturb the base stacking of DNA, unwind the DNA helix conformation, and lead to the loss of helicity [33]. Such a changing tendency is similar to the changes induced by cisplatin, which suggests that the covalent binding between Pt and DNA other than the groove binding mode might dominate the interactions between DNA and 1 [34]. Therefore 1 could bind to DNA through multiple binding modes involving non-covalent interaction and monofunctionalplatination of the platinum(II) moiety.

Interaction with protein (Figure 6)

Human serum albumin (HSA) is the most abundant protein present in the blood serum and plays many indispensable physiological roles, especially it serves as a transport protein for many intravenously administered drugs, such as platinum-based anticancer drugs [35,36]. Reaction between platinum-based drugs and HSA is considered to be one of important routes for the drugs in blood plasma [37,38]. Studies on the binding of plaitnum-based drugs to HSA in vitro can provide information on the structural feature that determines the therapeutic effectiveness of drugs and standardiezed screens for protein binding in new anticancer drug designs and for fixing dose limits [39]. Herein, the interaction of complex 1 with HSA was first studied by fluorescence spectroscopy. HSA possesses intrinsic fluorescence mainly resulting from the sole tryptophan residue (Trp-214) in the hydrophobic cavity of the protein [40]. The effect of complex 1 on the fluorescence emission spectra of HSA is shown in Fig. 6. As seen, the intensity of the characteristic broad emission band at about 350 nm of HSA decreased with increasing concentration of complex 1, which indicated that complex 1 could interact with HSA and quench its intrinsic fluorescence. The changes in the fluorescence intensity of Trp-214 in the presence of complex 1 may arise as a direct quenching or as a result of protein conformational changes induced by 1. In Figure 6, there is an obvious red shift (350 nm - 387 nm) of the maximum emission wavelength of HSA during the interaction, suggesting that the binding of complex 1 to HSA altered the microenvironment of the tryptophan residues, and the residues of HSA were placed in a more hydrophilic environment by interactions of 1 with HSA [41]. The result agrees with those obtained from the UV-vis absorption measurements Figure 7.

The UV-vis absorption spectra of HSA in the absence and presence of complex 1 are shown in Figure 7. HSA possesses two main absorption peaks around 208 nm and 278 nm. The strong absorption peak at about 208 nm originates from the $n \rightarrow \pi^*$ transition of HSA's characteristic polypeptide backbone structure C=O and is related to the changes in the conformation of the peptide backbone associated with the helix-coil transformation of HSA [42]. The week absorption peak at about 278 nm arises from the phenyl rings in the aromatic amino acid residues as Try, Tyr, and phenylalanine [43]. From Figure 7, it can be observed that with increasing amounts of 1 added to the HSA solution, the intensity of the absorption peak of HSA at 208 nm distinctly decreased with an obvious red shift (for 208 to 230 nm). The result indicates that the interaction between complex 1 and HSA lead to the loosening and unfolding of the protein skeleton. However, the intensity of the peak at 278 nm is generally increased by the addition of the complex, indicating that more aromatic acid residues are extended into the aqueous environment, and the tertiary structure of HSA is destroyed Figure 8(a) and Figure 8(b).

To investigate the quenching mechanism of HSA induced by complex 1, the fluorescence quenching data at different temperatures (291, 299, and 309 K) are analyzed according to the Stern-Volmer equation (eq. 2) and the modified Stern-Volmer equation (eq. 3) as follows [44]:

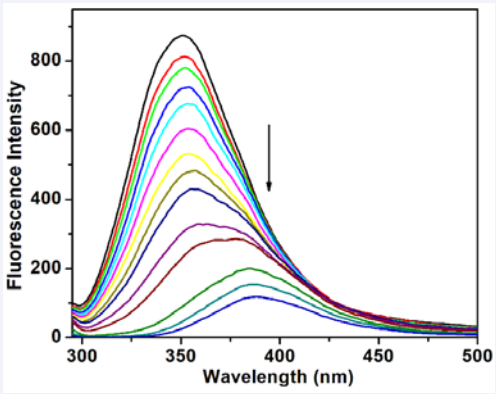

Figure 6 Fluorescence spectra of HSA (0.4 μM, λ_{ex} = 280 nm, λ_{em} = 351 nm) in the absence and presence of complex **1** (1.5, 3.0, 4.5, 6.0, 7.5, 9.0, 12.0, 15.0, 20.0, 30.0, 60.0, 90.0, 120 μM) at 191 K and pH 7.40.

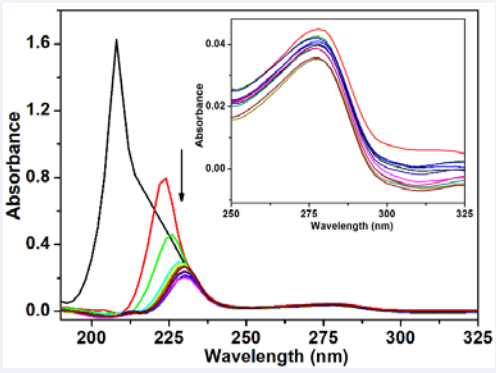

Figure 7 The UV-vis absorption spectra of HSA (1.0 μM, black line) in the absence and presence of increasing amounts of complex 1 (0.5, 1.0, 1.5, 2.0, 2.5, 3.0, 3.5, 4.0, 4.5, 5.0 μM) at 37 °C in pH 7.40 after 24 h of incubation time. In order to eliminate the absorption of complex 1 itself, an equal amount of 1 was subsequently used as reference.

$$\frac{F_0}{F} = 1 + K_{SV}[Q] = 1 + k_q \tau_0 [Q] \quad (2)$$

$$\frac{F_0}{F} = (1 + K_D[Q])(1 + K_S[Q]) = 1 + (K_D + K_S)[Q] + K_D K_S [Q]^2 \quad (3)$$

where F0 and F are the fluorescence intensities of HSA in the absence and presence of complex 1, respectively, [Q] is the concentration of complex 1, Ksv is the Stern-Volmer quenching constant, kq is the quenching rate constant of HSA, $\tau_0$is the average lifetime without complex 1 (τ_0 =10^{-8} s) [26], and KD and KS are the dynamic and static quenching constants, respectively. Figure 8 shows the plots of *F0/F* for HSA vs. [Q] of complex 1 ranging from 0 to 120μM and 0 to 15 M under various temperatures. Plots in Figure 8(a) show upward curvature towards the y-axis, and *F0/F* is related to [Q] by the modified Stern-Volmer equation (see eq. 3), which indicated that combined quenching (both dynamic and static) process was involved at higher concentration of complex 1 as discussed in the literature [4,45,46]. From Figure 8(b), it is clear that for lower concentration for complex 1, the Stern-Volmer curves are a good linear relationship. This suggests that the quenching type at lower complex concentrations was a single quenching mechanism, either static or dynamic [46]. Based on eq. 2, the calculated quenching constants and the rate constants at the corresponding temperature are listed in Table 2. As observed from Table 2, KSV increases with rising temperature, indicating that the fluorescence quenching of HSA by complex 1 is likely to occur via

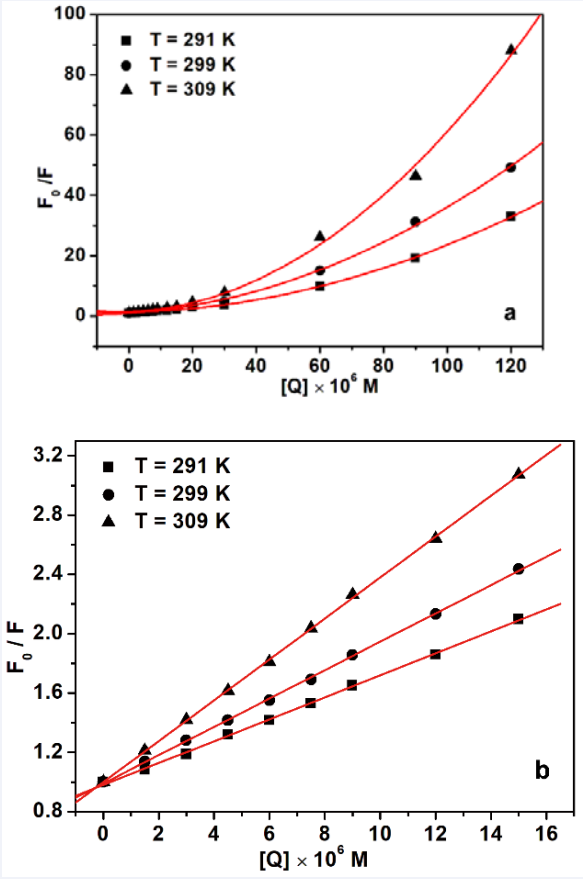

Figure 8 Stern-Volmer plots for the quenching of HSA (0.4 μM) by complex 1 ranging from 0 to 120 μM (a) and 0 to 15 μM (b) at different temperatures (291 K, 299 K, and 309 K) and pH 7.40.

Table 2: Stern-Volmer quenching contants (K_{sv}), quenching rate constants (k_q), binding constants (K_A) and number of binding sites (n) for the interaction of complex **1** with HSA at lower complex concentrations.

T (K)	K_{sv} × 10^{-5} (M^{-1})	k_q × 10^{-13} (M^{-1} s^1)	K_A × 10^{-5} (M^{-1})	n
291	0.74 ± 0.01	0.74 ± 0.01	0.84 ± 0.01	1.21
299	0.96 ± 0.02	0.96 ± 0.02	1.11 ± 0.02	0.94
309	1.38 ± 0.02	1.38 ± 0.02	1.76 ± 0.02	0.93

a dynamic quenching mechanism at lower complex concentrations. However, the values of kq are much higher than the maximum value (2.0×10^{10} $M^{-1}s^{-1}$) for diffusion-controlled quenching [39]. This result indicates that there is a specific interaction between the complex and HSA, and the probable quenching mechanism is not initiated by a dynamic process but by a static one (Table 2).

The binding parameters for the interaction of complex 1 and HSA were obtained by analyzing the fluorescence data. The apparent association constant KA and the number of binding sites n were calculated using the modified double logarithm regression equation (eq. 4) [47]:

$$\log \frac{F_0 - F}{F} = n \log K_A - n \log \left(\frac{1}{[Q_t] - (F_0 - F)[P_t]/F_0} \right) \quad (4)$$

where*F*0 and *F* are the fluorescence intensities in the absence and presence of complex 1, respectively, [Qt] and [Pt] are the total concentrations of complex 1 and HSA, respectively. Figure S5 shows the plot of log[$(F_0 - F)/F$] *versus* log{1/([Q_t] − (F_0 −*F*)[P_t]/F_0)}for the interaction between HSA and complex 1 at different temperatures, and the calculated values of KA and n are listed in Table 2. The association constants obtained are 10^5 M^{-1}, which are just at a moderate level [48]. The association constants increase with the temperature, suggesting that the interaction is an endothermic process [49]. The number of binding sites in HSA approximates to 1, indicating that only one site in HSA is reactive to complex 1. However, cisplatin can crosslink several residue sites on human albumin. Therefore, the interaction of HSA with complex 1 is relatively weaker than that with cisplatin (Figure 9(a), 9(b)).

Aiming to investigate the structural changes o pf HSA induced by complex 1, synchronous fluorescence spectra of HSA were measured before and after the addition of complex 1 to get valuable information on the molecular microenvironment, particularly in the vicinity of the fluorophore functional groups [39]. The impact of complex 1 on the synchronous fluorescence spectra of HSA at Δλ = 15 nm and Δλ = 60 nm is shown in Figure 9. The maximum emission wavelengths of tyrosine residue (about 285 nm) in HSA exhibited no notable red or hypsochromic shifts when Δλ= 15 nm, indicating that the microenvironment around the tyrosine residue did not undergo obvious changes during the binding process. However, the increasing concentration of the complex led to a significant red shift (from 279 to 284 nm) at the maximum emission peak of the tryptophan residue when Δλ = 60 nm, suggesting that the conformation of HSA was altered and the polarity around the tryptophan residues were placed in a less hydrophobic environment and more exposed to the solvent molecules during the interaction. Additionally, upon addition of complex 1 to HSA, the quenching of fluorescence intensity is observed for both Tyr and Trp residues with a concomitant increase in the fluorescence intensity of the Pt(II) complex (371 nm at Δλ=

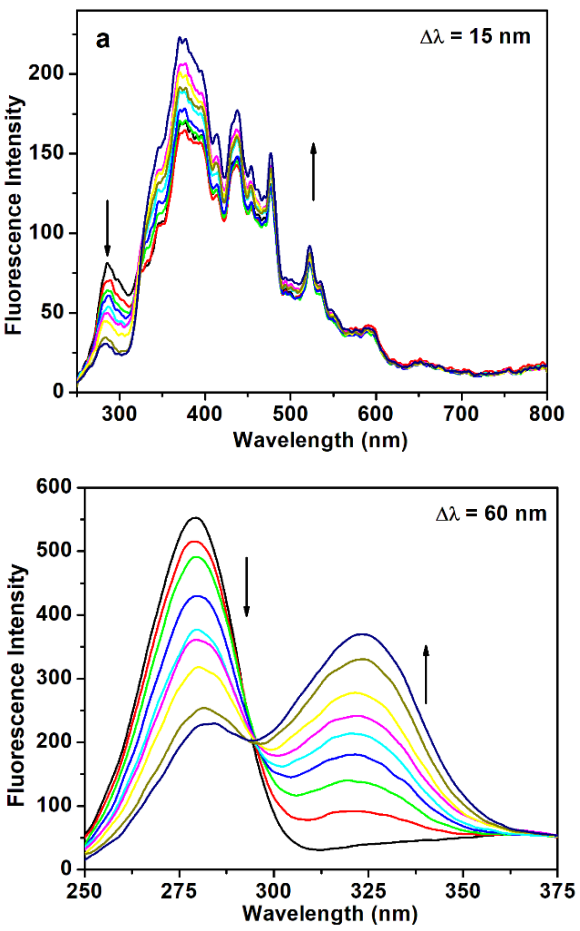

Figure 9 Impact of complex **1** (0, 1.5, 3.0, 4.5, 6.0, 7.5, 9.0, 12.0, 15.0 μM) on the synchronous fluorescence spectra of HSA (0.4 μM) at Δλ = 15 nm (a) and Δ = 60 nm (b).

15 nm; 325 nm at 60 nm, Figure S6). The obvious decrease in the fluorescence intensity between complex 1 and HSA may occur in domain II of HSA because both Tyr and Trp residues of HSA are located in this domain Figure 10.

To further confirm the conformational changes of HSA induced by complex 1, CD spectroscopy was performed. The CD spectra of HSA in the presence of complex 1 are shown in Fig. 10. As can be seen from Figure 10, HSA exhibits two negative bands at 208 and 222 nm in the ultraviolet region, which are characteristic of the typical α-helix structure of the protein [50]. The two negative bands contribute to the $\pi \rightarrow \pi^*$ and $n \rightarrow \pi^*$ transfers for the peptide bond of α-helical secondary structure content. This may imply that complex 1 is able to interact with the amino acid residues of the main polypeptide chain of HSA and destroy the hydrogen-bonding network. However, the CD spectra of HSA in the presence and absence of complex 1 are observed to be similar in shape, suggesting that the structure of HSA is predominantly α-helix even after binding.

CONCLUSION

In this study, we have prepared and characterized a novel benzothiazole-based mononuclear platinum(II) complex. The complex exhibited a cytotoxicity comparable to that of cisplatin against MCF-7 cell lines, and more potent activities against HeLa and A-549 cell lines. The complex could coordinate with N7-GMP and GSH to form the Pt-GMP adduct and Pt-GS complex, respectively. The coordination binding of 1 with GSH did not prevent the formation of a certain amount of the Pt-GMP adduct in the reaction process, which may be favorable in the clinical application of the complex. In addition, the complex could bind to human serum albumin (HSA) with a moderate binding affinity and quench the intrinsic fluorescence of HSA.

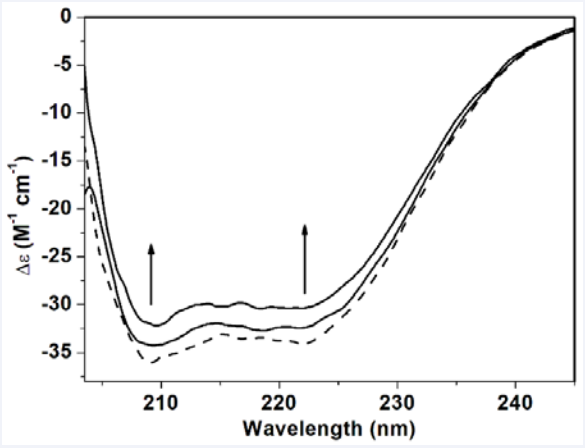

Figure 10 Far-UV CD spectra of HSA (0.3 μM) in the absence and presence of complex 1 (0, 5.0, and 10.0 μM, respectively, from the bottom to the top).

ACKNOWLEDGEMENT

We are grateful for financial supports from the National Natural Science Foundation of Hubei Province (No. 2018CFB658) and the Opening Project of Key Laboratory of Optoelectronic Chemical Materials and Devices, Ministry of Education, Jianghan University (No. JDGD-201810).

REFERENCES

1. Jamieson ER, Lippard SJ. Structure, Recognition, and Processing of Cisplatin-DNA Adducts. Chem Rev. 1999; 99: 2467-2510.
2. Kelland L.The resurgence of platinum-based cancer chemotherapy. Nat Rev Cancer.2007; 7: 573-584.
3. Chen ZF, Zhang SP, Zhang J, Zhu ZZ.Enhanced anti-cancer efficacy to cancer cells by a novel monofunctional mononuclear platinum (ii) complex containing a mixed S,N,S-donor ligand. New journal of chemistry. 2017; 41: 6760-6768.
4. Chen ZF, Zhang SP, Zhu ZZ, Zhang YM.A novel platinum (ii) anticancer complex of danyslbis(2-benzothiazolylmethyl)amine with dimethyl sulfoxide as a leaving group: synthesis, cytotoxicity, interaction with DNA and human serum albumin.New J Chem. 2017; 41: 6340-6348.
5. Ma ZD, Choudhury JR, Wright MW, Day CS, Saluta G, Kucera GL, et al. A Non-Cross-Linking Platinum-Acridine Agent with Potent Activity in Non-Small-Cell Lung Cancer. J Med Chem. 2008; 51: 7574-7580.
6. Keri RS, Patil MR, Patil SA, Budagumpi S. A comprehensive review in current developments of benzothiazole-based molecules in medicinal chemistry.Eur J Med Chem. 2015; 89: 207-251.
7. Bradshaw TD, Westwell AD. The development of the antitumourbenzothiazoleprodrug, Phortress, as a clinical candidate. Curr Med Chem. 2004; 11: 1009-1021.

8. Shi DF, Bradshaw TD, Wrigley S, McCall CJ, Lelieveld P, Fichtner I, et al. Antitumor Benzothiazoles. 3.1 Synthesis of 2-(4-Aminophenyl) benzothiazoles and Evaluation of Their Activities against Breast Cancer Cell Lines in Vitro and in Vivo. J Med Chem. 1996; 39: 3375-3384.

9. Tzanopoulou S, Pirmettis IC, Patsis G, Paravatou-Petsotas M, Livaniou E, Papadopoulos M, et al.Synthesis, Characterization, and Biological Evaluation of M(I)(CO)3(NNO) Complexes (M = Re, 99mTc) Conjugated to 2-(4-Aminophenyl)benzothiazole as Potential Breast Cancer Radiopharmaceuticals. J Med Chem. 2006; 49: 5408-5410.

10. Tzanopoulou S, Sagnou M, Paravatou-Petsotas M, Gourni E, Loudos G, Xanthopoulos S, et al. Evaluation of Re and 99mTc Complexes of 2-(4′-Aminophenyl)benzothiazole as Potential Breast Cancer Radiopharmaceuticals. J Med Chem. 2010; 53: 4633-4641.

11. Kim HK, Kang MK, Jung KH, Kang SH, Kim YH, Jung JC, et al.Gadolinium Complex of DO3A-benzothiazole Aniline (BTA) Conjugate as a Theranostic Agent. J Med Chem. 2013; 56: 8104-8111.

12. Dadmal TL, Appalanaidu K, Kumbhare RM, Mondal T, Ramaiah MJ, Bhadra MP. Synthesis and biological evaluation of triazole and isoxazole-tagged benzothiazole/benzoxazole derivatives as potent cytotoxic agents. New J Chem. 2018; 42: 15546-15551.

13. Jung Y, Lippard SJ. Direct Cellular Responses to Platinum-Induced DNA Damage. Chem Rev. 2007; 107: 1387-1407.

14. Krishnamoorthy P, Sathyadevi P, Butorac RR, Cowley AH, Bhuvanesh NSP, Dharmaraj N. Copper(i) and nickel(ii) complexes with 1 : 1 vs. 1 : 2 coordination of ferrocenylhydrazone ligands: Do the geometry and composition of complexes affect DNA binding/cleavage, protein binding, antioxidant and cytotoxic activities?. Dalton Trans. 2012; 41: 4423-4436.

15. Groessl M, Terenghi M, Casini A, Elviri L, Lobinski R, Dyson PJ. Reactivity of anticancer metallodrugs with serum proteins: new insights from size exclusion chromatography-ICP-MS and ESI-MS. J Anal AtSpectrom. 2010; 25: 305-313.

16. Matouzenko GS, Bousseksou A, Lecocq S, Koningsbruggen PJ, van Perrin M, Kahn O, Collet A. spin transition in [Fe(DPEA)(NCS)2], a compound with the new tetradenate ligand (2-aminoethyl)bis(2-pyridylmethyl)amine(DPEA): crystal structure, magnetic properties, and Mossbauer spectroscopy.1997 Inorg Chem. 36:2975-2981.

17. Price JH, Schramm RF, Wayland BB, Williams A. Palladium(II) and platinum(II) alkyl sulfoxide complexes. Examples of sulfur-bonded, mixed sulfur- and oxygen-bonded, and totally oxygen-bonded complexes. Inorg Chem. 1972; 11: 1280-1284.

18. ISOPRO 1998 Mike Senko, 243 Buena Vista Ave. #502, Sunnyvale, CA 94086, USA.

19. Reichmann ME, Rice SA, Thomas CA, Doty P.A further examination of the molecular weight and size of de pentose nucleic acid. J Am Chem Soc.1954; 76: 3047-3053.

20. Baldini M, Belicchi-Ferrai M, Bisceglie F, Pelosi G, Pinelli S, Tarasconi P.Cu(II) Complexes with Heterocyclic Substituted Thiosemicarbazones: The Case of 5-Formyluracil. Synthesis, Characterization, X-ray Structures, DNA Interaction Studies, and Biological Activity. Inorg chem. 2003; 42: 2049-2055.

21. Fichtinger-Schepman AM, van der Veer JL, den Hartog JH, Lohman PH, Reedijk J. Adducts of the antitumor drug cis-diamminedichloroplatinum(II) with DNA: formation, identification, and quantitation. Biochemistry. 1985; 24: 707-713.

22. Wang XY, Guo ZJ. The role of sulfur in platinum anticancer chemotherapy. Anti-cancer Agents Med Chem. 2007; 7: 19-34.

23. Hochreuther S, van Eldik R 2012 InorgChem 51:3025-3038

24. Mahadevan S, Palaniandavar M. Spectroscopic and Voltammetric Studies on Copper Complexes of 2,9-Dimethyl-1,10-phenanthrolines Bound to Calf Thymus DNA. Inorg Chem. 1998; 37: 693-700.

25. LePecq JB, Paoletti C. A fluorescent complex between ethidium bromide and nucleic acids. Physical-chemical characterization. J Mol Biol. 1967; 27: 87-106.

26. Lakowicz JR, Weber G. Quenching of fluorescence by oxygen. Probe for structural fluctuations in macromolecules. Biochemistry. 1973; 12: 4161-4170.

27. Haworth IS, Elcock AH, Freemann J, Rodger A, Richards WGJ. Sequence Selective Binding to the DNA Major Groove: Tris(1,10-phenanthroline) Metal Complexes Binding to Poly(dG-dC) and Poly(dA-dT) J BiomolStructDyn. 1991; 9: 23-43.

28. Maity B, Roy M, Saha S, Chakravarty AR. Photoinduced DNA and Protein Cleavage Activity of Ferrocene-Conjugated Ternary Copper(II) Complexes. Organometallics. 2009; 28: 1495-1505.

29. Cory M, McKee DD, Kagan J, Henry DW, Miller JA.Design, synthesis, and DNA binding properties of bifunctionalintercalators. Comparison of polymethylene and diphenyl ether chains connecting phenanthridine. J Am Chem Soc. 1985; 107: 2528-2536.

30. Sheng X, Lu XM, Chen YT, Luo GY, Zhang JJ, Shao Y, et al. Synthesis, DNA-Binding, Cleavage, and Cytotoxic Activity of New 1,7-Dioxa-4,10-diazacyclododecane Artificial Receptors Containing Bisguanidinoethyl or Diaminoethyl Double Side Arms. ChemEur J. 2007; 13: 9703-9712.

31. Johnson JR in Circular Dichroism: Principles and Application, ed. Nakanishi K, Berova N, Woody RW, VCH, New York, 1994; 523.

32. Madureira J, Ramos CIV, Marques M, Maia C, Sousa B, Campino L, et al. NonclassicMetallointercalators with Dipyridophenazine: DNA Interaction Studies and Leishmanicidal Activity. Inorg Chem. 2013; 52: 8881-8894.

33. Karidi K, Garoufis A, Hadjiliadis N, Reedijk J. Dalton Trans. 2005; 723-734.

34. Gay M, Montana AM, Batalla C, Mesas JM, Alegre MT. Design, synthesis and SAR studies of novel 1,2-bis(aminomethyl)cyclohexane platinum(II) complexes with cytotoxic activity. Studies of interaction with DNA of iodinated seven-membered 1,4-diaminoplatinocycles. J InorgBiochem. 2015; 142: 15-27.

35. Kabir MZ, Mukarram AK, Mohamad SB, Alias Z, Tayyab S. Characterization of the binding of an anticancer drug, lapatinib to human serum albumin. J PhotochemPhotobiol B. 2016; 160: 229-239.

36. Chanphai P, Vesper AR, Bariyanga J, Bérubé G, Tajmir-Riahi HA. Review on the delivery of steroids by carrier proteins. J Photochem Photobiol B. 2016; 161: 184-191.

37. Messori L, Merlino A. Cisplatin binding to proteins: A structural perspective. CoordChem Rev. 2016; 315: 67-89.

38. Shahabadi N, Hadidi S, Kalar ZM. Biophysical studies on the interaction of platinum(II) complex containing antiviral drug ribavirin with human serum albumin. J PhotochemPhotobiol B. 2016; 160: 376-382.

39. Samari F, Hemmateenejad B, Shamsipur M, Rashidi M, Samouei H. Affinity of Two Novel Five-Coordinated Anticancer Pt(II) Complexes to Human and Bovine Serum Albumins: A Spectroscopic Approach. Inorg Chem. 2012; 51: 3454-3464.

40. Abou-Zied OK, Al-Shihi OIK. Characterization of Subdomain IIA Binding Site of Human Serum Albumin in its Native, Unfolded, and Refolded States Using Small Molecular Probes. J Am Chem Soc. 2008; 130: 10793-10801.

41. Yuan T, Weljie AM, Vogel HJ. Tryptophan Fluorescence Quenching by Methionine and Selenomethionine Residues of Calmodulin:

Orientation of Peptide and Protein Binding. Biochemistry. 1998; 37: 3187-3195.

42. Polet H, Steinhardt J. Binding-induced alterations in ultraviolet absorption of native serum albumin. Biochemistry. 1968; 7: 1348-1356.

43. Li Y, He WY, Xue CX, Hu ZD, Chen XG, Sheng FL. Effect of Chinese medicine alpinetin on the structure of human serum albumin.Bioorg Med Chem. 2005; 13: 1837-1845.

44. Lakowicz JR. Quenching of fluorescence. In: Lakowicz JR, ed. Principles of fluorescence spectroscopy, Springer, New York. 3: 2006.

45. Li DJ, Zhang T, Xu C, Ji BM. Effect of pH on the interaction of vitamin B12 with bovine serum albumin by spectroscopic approaches. SpectrochimActa Part A. 2011; 83: 598-608.

46. Eftink MR, Ghiron CA. Fluorescence quenching of indole and model micelle systems. J Phys Chem. 1976; 80: 486-493.

47. Bi SY, Song DQ, Tian Y, Zhou X, Liu ZY, Zhang HQ.Molecular spectroscopic study on the interaction of tetracyclines with serum albumins. SpectrochimActa Part A. 2005; 61: 629-636.

48. Tolia C, Papadopoulos AN, Raptopoulou CP, Psycharis V, Garino C, Salassa L, et al. Copper(II) interacting with the non-steroidal antiinflammatory drug flufenamic acid: Structure, antioxidant activity and binding to DNA and albumins. J InorgBiochem. 2013; 123: 53-65.

49. Wang YQ, Wang XY, Wang J, Zhao YM, He WJ, Guo ZJ. Noncovalent Interactions between a TrinuclearMonofunctional Platinum Complex and Human Serum Albumin. Inorg Chem. 2011; 50: 12661-12668.

50. Ibrahim N, Ibrahim H, Kim S, Nallet JP, Nepveu F.Interactions between Antimalarial Indolone-N-oxide Derivatives and Human Serum Albumin.Biomacromolecules. 2010; 11: 3341-3351.

Cite this article

Chen Z, Wu Y, Zhang Q, Zhang Y (2020) Biological Properties of a Benzotiazole-Based Mononuclear Platinum(II) Complex as a Potential Anticancer Agent. JSM Clin Case Rep 8(1): 1173.